

RESEARCH

Open Access



CDH4 inhibits ferroptosis in oral squamous cell carcinoma cells

Jian Xie^{1,2†}, Ting Lan^{1†}, Da-Li Zheng¹, Lin-Can Ding^{1*} and You-Guang Lu^{1,2*}

Abstract

Background The cadherin-4 gene (CDH4), a member of the cadherin family genes, encodes R-cadherin (R-cad); however, the function of this gene in different types of cancer remains controversial. The function of CDH4 in OSCC (oral squamous cell carcinoma) is unknown.

Materials and methods We use the Cancer Genome Atlas (TCGA) database to find the expression of CDH4 in OSCC is more than normal tissue. Our tissue samples also confirmed that CDH4 gene was highly expressed in OSCC. The related cell function assay detected that CDH4 promotes the ability of cell proliferation, migration, self-renewal and invasion. Cell staining experiment confirmed that the change of CDH4 expression would change the cell mortality. The western blot of GPX4 (glutathione-dependent peroxidase-4), GSH (reduced glutathione) test assay and MDA (Malondialdehyde) test assay show that the expression of CDH4 may resist the sensitivity of ferroptosis in OSCC.

Results CDH4 was upregulated in OSCC samples and was correlation with poor survival of patients. High expression of CDH4 effectively promotes the proliferation, mobility of OSCC cells and reduce the sensitivity of OSCC cells to ferroptosis. CDH4 is positively correlated with EMT pathway genes, negatively correlated with fatty acid metabolism pathway genes and peroxisome pathway genes, and positively correlated with ferroptosis suppressor genes in OSCC.

Conclusions These results indicate that CDH4 may play a positive role in tumor progression and resistance ferroptosis and may be a potential therapeutic target for OSCC.

Keywords CDH4, R-cadherin, Ferroptosis, Oral squamous cell carcinoma

Introduction

The cadherin family consists of classical intercellular adhesion molecules that are Ca²⁺-dependent [1, 2]. The extracellular domain of cadherin binds to catenin, and

is connected to the cytoskeleton, thus forming cell–cell adhesions (AJs). AJs is the most common and universal type of cell adhesion [3]. Therefore, cadherin is necessary for the stability of intercellular adhesion and normal cell physiological activities. It is related to cell–cell adhesion, cell growth, cell polarity, cell motility, differentiation and survival [4–6]. When cells undergo malignant transformation, the destruction of cell adhesion will help tumor cells to invade and metastasize. Some studies believe above changes must be related to cadherin, AJs or activating some signal pathways [7–12]. CDH4 is a member of the cadherin family and encodes R-cadherin. CDH4 plays an important role in the differentiation of retina, kidney, striated muscle and brain nerves [13–17]. It also is found to be associated with the occurrence and

[†]Jian Xie and Ting Lan contributed equally to this work.

*Correspondence:

Lin-Can Ding
lincanding@fjmu.edu.cn

You-Guang Lu
fjlyg63@fjmu.edu.cn

¹ Department of Preventive Dentistry, School and Hospital of Stomatology, Fujian Medical University, 246 Yang Qiao Middle Road, Fuzhou 350002, China

² Key Laboratory of Stomatology of Fujian Province, School and Hospital of Stomatology, Fujian Medical University, 88 Jiaotong Rd, Fuzhou 350004, China



Table 1 The primers for real-time PCR

Gene	Accession no	Forward	Reverse
ACTB	NM0011101	CCTGGCACCCAGCACAAT	GGGCCGGACTCGTCATACT
CDH4	NM001794.2	CGTCCATCATCAAAGTCAAGGT	GGTCGTAGTCCTGGTCTCTCT

Table 2 The siRNA and negative control sequences for CDH4

Name	Sequence	
siRNA-1	5'-CGUCCAUCAUCAAGUCAATT-3'	5'-UUGACUUUGAUGAUGGACGTT-3'
siRNA-2	5'-GCGACAACAUCUCAAGUATT-3'	5'-UACUUGAGGAUGUUGUCGCTT-3'
NC	5'-UUCUCCGAACGUGUCACGUTT-3'	5'-ACGUGACACGUUCGGAGAATT-3'

metastasis of a variety of tumors, but its function in different types of cancer is controversial [18–27].

Ferroptosis is a new cell death pattern discovered by Dixon in 2012 [28]. It is a programmed cell death, which is mainly caused by lipid peroxidation of mitochondrial membrane due to iron-dependent ROS (reactive oxygen species) accumulation in cells [29]. Ferroptosis is considered to have three classical pathways, GPX4 regulation pathway, iron metabolism pathway and lipid metabolism pathway [30]. Ferroptosis has been found in many kinds of cancer and is considered as the key mechanism of tumor treatment research [31, 32]. Tumor cells require more iron to maintain vigorous growth than normal cells, ferroptosis is considered to be an adaptive mechanism to eliminate malignant cells, especially in tumor cell lines that have developed resistance to chemotherapy drugs [33–35].

OSCC is a common cancer worldwide, especially in South Asia. It is an important part of HNSCC (head and neck squamous cell carcinoma). There were approximately 377,713 new cases of OSCC and 17,757 new deaths in 2021. OSCC is the eighth most common cancer among men, and it has the highest incidence in Asia [36]. New cases of OSCC account for 3% of all new cancer cases, and deaths from OSCC account for 1.8% of all deaths in the United States [37]. OSCC has a poor five-year overall survival rate of 40%–50%, and the survival rate of advanced cancer patients is only 20% [38, 39]. The conventional treatment of OSCC is surgery,

radiation therapy and chemotherapy, often combination therapy. The variability of patients' response to OSCC treatment is relatively high, and the recurrence rate of OSCC is as high as 50% [40]. Current treatments are frequently ineffective and severely affect patient quality of life [41].

Despite the development of study and treatments, overall survival has not improved significantly over the past 20 years [42]. The poor prognosis of this disease is due to a propensity for recurrence and distant metastasis [43]. At present, for the treatment of OSCC, some studies start with precancerous lesions [44, 45], some study the application of compound Chinese medicine [46], some study the optimization of chemotherapy drug delivery routes [47], and some are keen to find molecular targets for the diagnosis and treatment of oral cancer [48–50]. However, the function of CDH4 gene in OSCC and its relationship with ferroptosis are unknown. In this study, we investigated the role of CDH4 and its relationship with ferroptosis in OSCC. To study the possibility of CDH4 gene as a target for diagnosis and treatment.

Materials and methods

Cell lines and cell culture

The CAL27, HN30, HN6 and SCC9 cell lines were purchased from ATCC (American Type Culture Collection, USA). CAL27, HN30 and HN6 cells were grown in high-glucose DMEM (Gibco BRL, Grand Island, NY, USA) supplemented with 10% FBS (Gibco BRL, Grand Island,

(See figure on next page.)

Fig. 1 CDH4 is upregulated in OSCC. The expression of CDH4 is different in many kinds of cancers in the TCGA database (A). Compared with normal tissues adjacent to cancer, CDH4 is highly expressed in HNSCC tissues in unpaired samples (B, $P < 0.01$) and paired samples (C, $P < 0.001$). The overall survival rate was higher in the CDH4-low-expression group than in the CDH4-high-expression group (D, $P = 0.074$). CDH4 is highly expressed in OSCC tissues in unpaired samples (E, $P < 0.01$) and paired samples (F, $P < 0.01$). The overall survival rate was higher in the CDH4-low-expression group than in the CDH4-high-expression group (G, $P = 0.133$). CDH4 is highly expressed in our clinical OSCC paired samples (H, $P < 0.05$). (* indicates $P < 0.05$, ** indicates $P < 0.01$, *** indicates $P < 0.001$, **** indicates $P < 0.0001$)

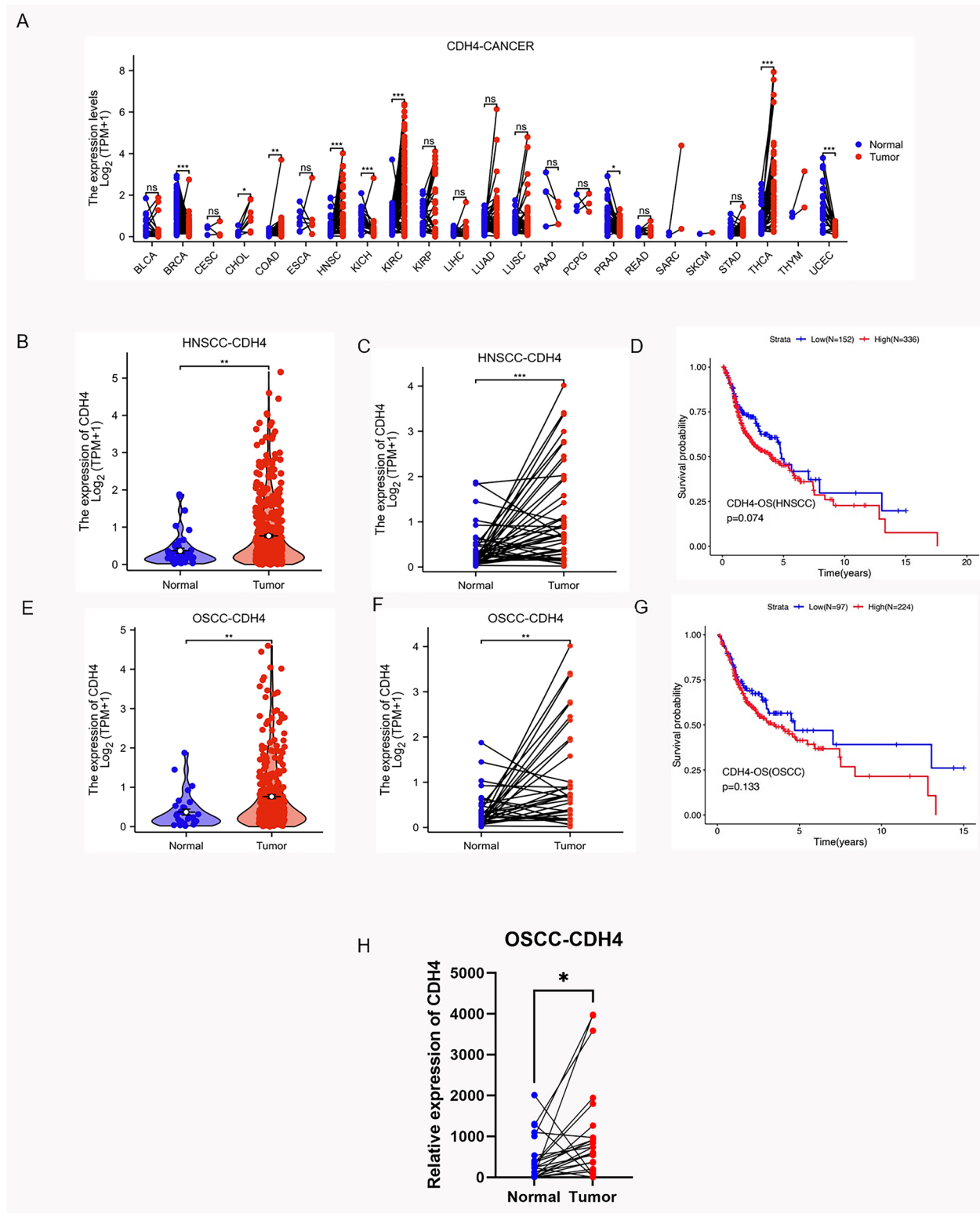


Fig. 1 (See legend on previous page.)

NY, USA). SCC9 cells were grown in DMEM/F-12 (Gibco BRL, Grand Island, NY, USA) supplemented with 10% FBS. All cells were incubated in a humidified atmosphere containing 5% CO₂ at 37 °C.

Acquisition of tissue samples

Fresh samples of 22 patients with oral squamous cell carcinoma and normal tissues adjacent to cancer were obtained from the First Affiliated Hospital of Fujian Medical University. According to the guidelines of Helsinki Declaration, the behavior was informed by each patient and provided with a written informed consent. The study was approved by the Ethics Committee of the Fujian Medical University, ethical number 2021-FMUSS-024.

Real-time quantitative RT-PCR (qPCR)

Nucleozol Reagent (Invitrogen, USA) was used to extract total RNA from 3 × 10⁵ HN30 and SCC9 cells cultivated in six-well plates. Total RNA was reverse transcribed to cDNA using the PrimeScript™ RT reagent kit (Takara, Japan). Real-time PCR was performed with SYBR GREEN Supermix (BIO-RAD, USA) using the following program: initial denaturation at 94 °C for 10 min, followed by 40 cycles of 94 °C for 15 s and 60 °C for 45 s. Data were analyzed according to the 2^{-ΔΔCT} method. The sequences of CDH4 and ACTB are listed in Table 1.

Design and synthesis of corresponding siRNAs and CDH4 overexpression vector

To target different coding regions of CDH4, three corresponding siRNAs were designed and synthesized (Shanghai GenePharma Co., Shanghai, China). The sequence information is presented in Table 2. All siRNAs were separately transfected into HN30 and SCC9 cells using Lipofectamine® RNAmate Transfection Reagent (Invitrogen, USA) following the manufacturer's instructions. The pcDNA3.1-FLAG-CDH4 plasmid and pcDNA3.1-vector plasmid was designed and synthesized by (Shanghai GenePharma Co., Shanghai, China). were separately transfected into HN30 and SCC9 cells using Lipofectamine™ 2000 Transfection Reagent (Invitrogen, USA).

Western blotting

Total protein was separated by 8% SDS-PAGE and transferred onto PVDF membranes (Amersham, USA). The membranes were blocked in 1% bovine serum albumin and incubated with primary antibodies against R-cad (Abnova Cat# PAB1864) at a dilution of 1:500 at 4 °C for 10 h, Gapdh (Cell Signaling Technology Cat# 51,332) at a dilution of 1:1000 at 4 °C for 10 h, β-actin (Cell Signaling Technology Cat# 5125) at a dilution of 1:1000 at 4 °C for 10 h, Flag and GPX4 (Cell Signaling, USA, Cat#52,455) at a dilution of 1:1000 at 4 °C for 10 h. When the expected bands, estimated by the molecular weight ladder and the manufacturer's instructions of primary antibodies, were separated enough, the blots were cut into 2 or 3 parts prior to incubation with primary antibodies. The original gels and multiple exposure images were shown in Supplementary Fig. 1.

TCGA database, Hallmark gene set and ferroptosis database

The transcript data and clinical information from the HNSCC and OSCC datasets were downloaded from the TCGA database (<http://gdc.cancer.gov>). The data were obtained on March 8th, 2023, and the HNSCC dataset contained 504 HNSCC samples and 44 normal tissues adjacent to cancer. The OSCC samples contained 330 cancer samples and 32 normal tissues adjacent to cancer. Hallmark gene set from MSigDB (Molecular signatures database) was used to GESA to find the related genes and pathways. The data of ferroptosis gene comes from the ferroptosis database (zhounan.org/ferrdb).

In vitro cell proliferation assay

Cell proliferation was evaluated by colony formation assay and counting of viable cells using the Cell Counting Kit-8 (CCK-8, Dojindo, Kumamoto, Japan). In the colony formation assay, 3 × 10³ cells (CDH4 knockdown experiment) and 1.5 × 10³ cells (CDH4 overexpression experiment) were plated in each well of a 6-well plate and cultivated for 2 weeks. After forming visible clones, the cells were stained with crystal violet, and the number of

(See figure on next page.)

Fig. 2 Knockdown of CDH4 suppresses the proliferation and stemness of OSCC. The expression of CDH4 in four kinds of OSCC cells **A-B**. CDH4 expression was effectively reduced by siRNAs as measured by real-time PCR **C** and western blot **D** in HN30 cells. CDH4 expression was effectively reduced by siRNAs as measured by real-time PCR **E** and western blot **F** in SCC9 cells. After transfection with CDH4 siRNAs, the growth of HN30 cells **G** and SCC9 **H** cells was measured by CCK-8 assay. The colony formation assay showed that the proliferation of HN30 cells **I** and SCC9 cells **J** was decreased after CDH4 knockdown. The number of colonies was counted. The picture shows the cell sphere formation in different groups under a 40X microscope **K**, and the number of spheres was decreased in the siRNA-1 and siRNA-2 groups compared with the NC group **L**. These experiments were repeated three times. (* indicates $P < 0.05$, ** indicates $P < 0.01$, *** indicates $P < 0.001$, **** indicates $P < 0.0001$, Values are presented as means ± standard error.)

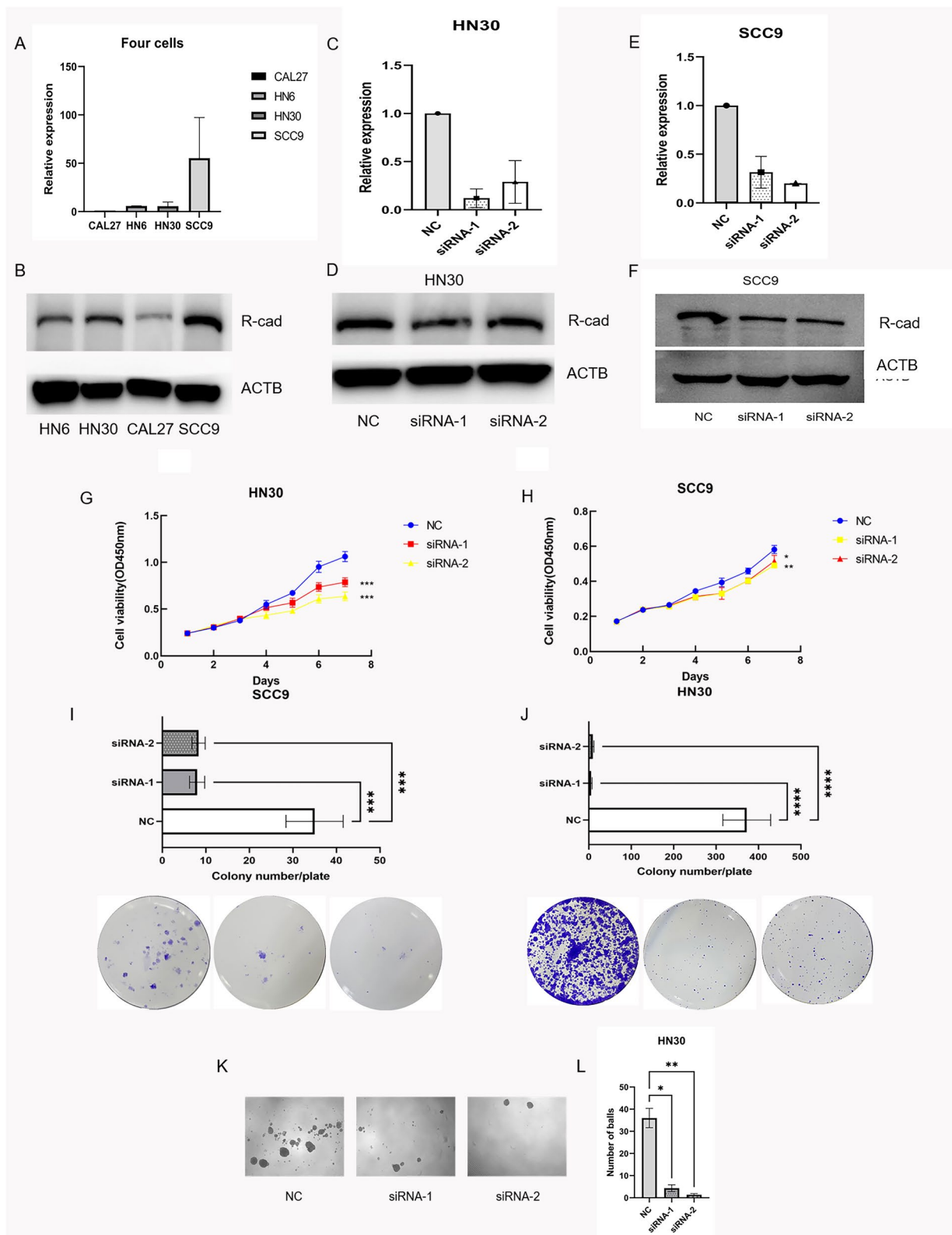


Fig. 2 (See legend on previous page.)

clones was counted. The experiments were conducted in triplicate and repeated three times. In the CCK-8 assay, first, the cells were transfected with siRNA and then plated into a 96-well plate at a rate of 3×10^3 per well and CDH4 overexpression cells plated into a 96-well plate at 1.5×10^3 per well. The wells were monitored daily and observed continually for 6 or 7 days. CCK-8 reagent (10 μ l) was added to the medium, and the plates were incubated for 1 h. The absorption at 450 nm was measured at the same time every day for 6 consecutive days.

In vitro cell invasion assay

Cell invasion was evaluated by a transwell invasion assay using 24-well Matrigel-coated Transwell chambers (8- μ m pore size, BD, USA). The HN30 cells were evenly plated at 1×10^5 cells/well in DMEM without FBS in the upper chamber and DMEM containing 10% FBS in the lower chamber in CDH4 knockdown experiment. The HN30 cells were evenly plated at 8×10^5 cells/well in DMEM without FBS in the upper chamber in CDH4 overexpression experiment. The SCC9 cells were plated at 5×10^4 cells/well in the upper chamber. After incubation at 37 °C for 48 h, Matrigel and cells on the upper chamber were removed with cotton swabs, and the cells were stained with crystal violet for 10 min. Cells were counted and photographed under a microscope in at least five random fields.

In vitro cell migration assay

Cell migration was evaluated using transwell migration and wound-healing assays. The method of the transwell migration assay was similar to that of the transwell invasion assay, but the transwell chambers without Matrigel (8- μ m pore size, BD, USA). In the upper chamber, HN30 cells were plated at 8×10^4 cells/well in CDH4 knockdown experiment and plated at 6×10^4 cells/well in CDH4 overexpression experiment, and SCC9 cells were plated at 4×10^4 cells/well. For wound-healing assays, the transfected cells were plated in a 12-well plate, and when the cells were spread onto the bottom of the dish, a trace was drawn evenly. After scratching, the culture medium was changed to serum-free DMEM. Gap areas were photographed at different time points using a light microscope (40X).

Cancer stem cell sphere culture

OSCC cells were collected, and serum was removed. HN30 cells were suspended in serum-free DMEM and stem cell medium (STEMCELL Technologies Inc., Catalog # 05926) at a ratio of 1:1. The cells were cultured in 96-well plates in ultralow attachment dishes (Corning Life Sciences, Catalog#3262). HN30 cells were seeded at a density of 1000 cells/100 μ l in CDH4 knockdown experiment and seeded at a density of 500 cells/100ul in CDH4 overexpression experiment. After two weeks of cultivation, the spheres of cells were statistically analyzed.

Live and dead cell staining

Live and dead cell staining was performed using a Calcein-AM/PI assay kit (Solarbio, China). Treated cells were stained with calcein-AM solution (1:1000) and incubated at 37°C for 20 min, then added PI solution (3:1000) incubated at 37°C for 5 min. The numbers of live and dead cells were detected under a laser confocal scanning microscope (OLYMPUS IX83, USA). The live cells fluoresced green (Calcein-AM staining), and the dead cells fluoresced red (PI staining). Under 400X magnification, 6 fields of view were taken for each hole.

GSH/GSSG detection experiment and MDA test assay

GSH/GSSG in cells was detected by a GSH and GSSG Assay Kit (Beyotime, China). Cells transfected for 48 h were treated with this kit and added to 96-well plate incubated for 30 min to detect GSH. The absorption was detected at 412 nm. MDA is tested by MDA test assay kit (Beyotime, China). Cells transfected for 48 h were treated with extracting solution in ultrasonic 7 min (work for 3 s and rest for 10 s in each time). The supernatant of cells was obtained after centrifugation 10,000 rpm 10 min. The supernatant was added corresponding reagents, incubated at 100°C for 1 h and centrifugated at 8000 rpm 10 min. The final supernatant was added 200ul to each well into 96-well plate.

The absorption was detected at 532 nm and 600 nm.

Statistical analysis

The experimental data were analyzed and graphed by GraphPad Prism 9 (GraphPad Software, USA). Paired Clinical samples were tested by Wilcoxon signed rank

(See figure on next page.)

Fig. 3 Knockdown of CDH4 suppresses the motility of OSCC. In the transwell migration assay and transwell invasion assay, the number of cells that passed through the filters was counted for HN30 cells **A–B** and SCC9 cells **D–E**. Representative images show the cells transfected with CDH4 that passed through the upper chamber of the transwell with and without (upper panel) Matrigel coating for HN30 cells **C** and SCC9 cells **F**. The numbers of migrating and invading cells were counted from at least five randomly selected fields of view under a microscope at 100X magnification. For the wound-heal assay, the representative images show the distances of cells passing through the scratch within a period of time for HN30 cells **G** and SCC9 cells **I** under a 40X microscope field of view. The mobility rate of cells was measured for HN30 cells **H** and SCC9 cells **J**. These experiments were repeated three times. (* indicates $P < 0.05$, ** indicates $P < 0.01$, *** indicates $P < 0.001$, **** indicates $P < 0.0001$, Values are presented as means \pm standard error)

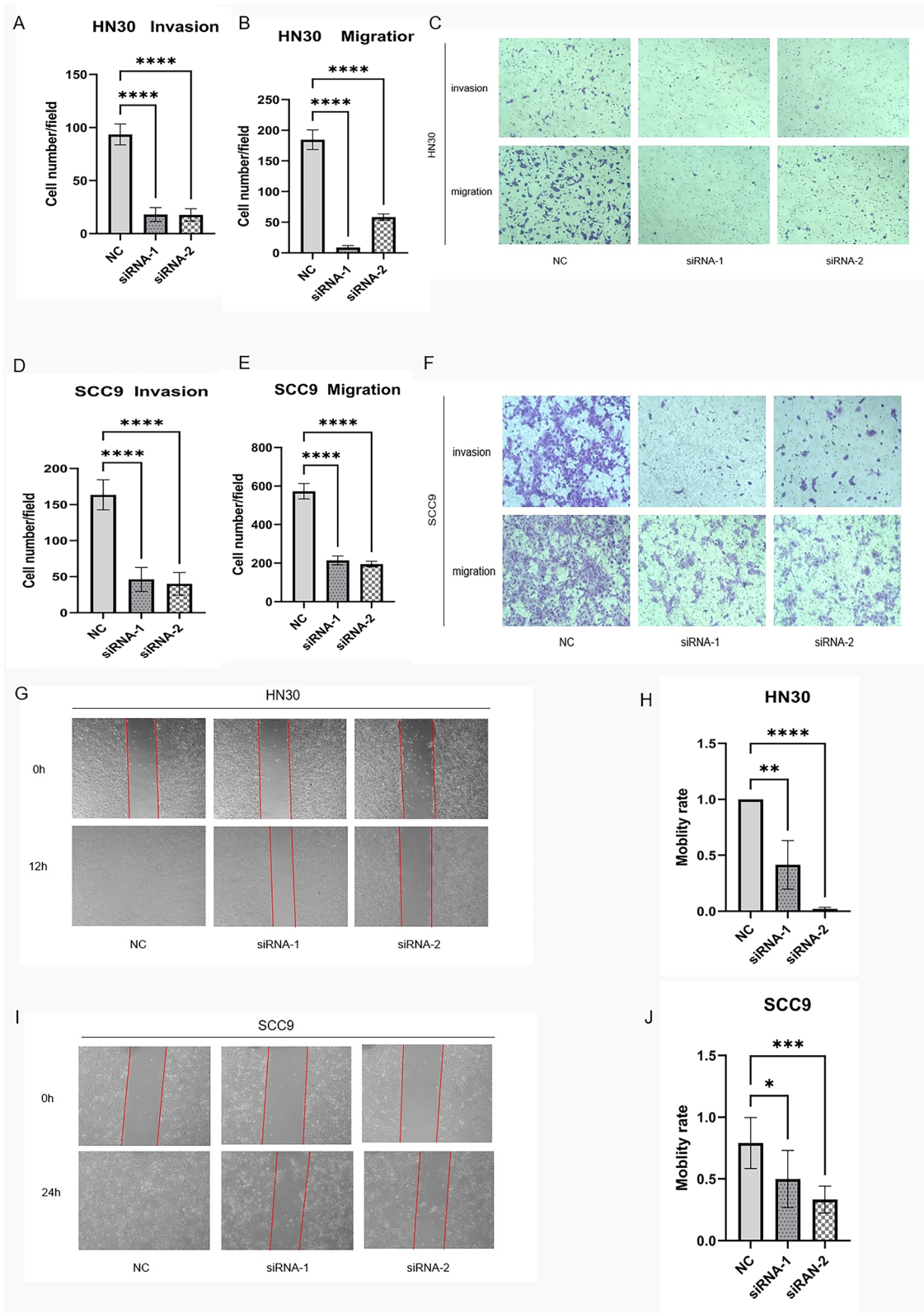


Fig. 3 (See legend on previous page.)

test and unpaired samples were tested by Wilcoxon rank sum test. Overall survival was tested by Km plot log-rank test. Genes correlation analysis was tested by person or spearman test. Comparisons between two groups were performed using two tailed unpaired t test and comparisons among three groups were performed using one-way analysis of variance. In the graphs, ns indicated $P > 0.05$, while $P < 0.05$ was considered statistically significant (* indicates $P < 0.05$, **indicates $P < 0.01$, ***indicates $P < 0.001$, ****indicates $P < 0.0001$, Values are presented as means \pm standard error.).

Results

CDH4 is upregulated in OSCC

In order to study the function of CDH4 in OSCC, we used the data of tumor samples given by TCGA to analyze the expression of CDH4 in different tissues and the relationship between CDH4 expression and overall survival rate of patients. OSCC is an important part of head and neck squamous cell carcinoma (HNSCC), we have analyzed the samples from HNSCC and OSCC, hoping to get hints through as many samples as possible. After the database sample analysis, we also analyzed the samples of 22 patients' OSCC tissues and normal tissues adjacent to cancer obtained from the First Affiliated Hospital of Fujian Medical University to further clarify the expression of CDH4 in OSCC.

The chart shows the differential expression of CDH4 between cancer and normal tissues adjacent to the cancer in the TCGA database (Fig. 1A). We found that the expression of CDH4 is higher in cholangiocarcinoma (CHOL), Colon adenocarcinoma (CAOD), KIRP (Kidney renal papillary cell carcinoma), KIRC (Kidney renal clear cell carcinoma), THCA (Thyroid carcinoma) and HNSCC than normal tissues adjacent to the cancer. In HNSCC, the CDH4 is more highly expressed than in adjacent normal tissues (Fig. 1B). More highly expressed in cancer tissues than in normal adjacent cancer tissues in 43 paired samples (Fig. 1C). The median overall survival of patients, in

the CDH4-high-expression group was shorter than that in the CDH4-low-expression group in HNSCC, but the difference is not significant enough (Fig. 1D). In OSCC, the CDH4 is more highly expressed in cancer tissues than in normal tissues (Fig. 1E) and more highly expressed in cancer tissues than in normal adjacent cancer tissues in the same patient (Fig. 1F) in 32 paired samples. The median overall survival of patients, in the CDH4-high-expression group was shorter than that in the CDH4-low-expression group in OSCC, but the difference is not significant enough (Fig. 1G). We extracted RNA from fresh clinical OSCC samples and detected the expression of CDH4 in the samples by real-time PCR. The expression of CDH4 is higher in OSCC group than in normal adjacent cancer tissues in 22 paired samples of our OSCC samples (Fig. 1H). We analyzed the expression of CDH4 in HNSCC and OSCC in the database, and combined with the analysis of CDH4 in our own tissue samples, we found that the expression of CDH4 is higher in cancer tissues than in normal tissues adjacent to cancer, which may remind that CDH4 promotes the occurrence and development of OSCC.

Downregulation of CDH4 expression suppressed the proliferation and stemness of OSCC cells in vitro

Firstly, we investigated whether CDH4 is related to the proliferation and self-renewal ability of OSCC. Among the four OSCC cell lines, higher expression levels of CDH4 were seen in the HN30 and SCC9 cell lines than in the HN6 and CAL27 cell lines (Fig. 2A-B). To detect the function of CDH4 in the proliferation of OSCC cells, two siRNAs targeting CDH4 were transfected into SCC9 and HN30 cells to knockdown CDH4 expression. Realtime-PCR and western blotting showed that the CDH4 gene was significantly downregulated in HN30 (Fig. 2C-D) and SCC9 cells (Fig. 2E-F). Changes in cell proliferation ability were observed after downregulation of CDH4. CCK-8 assays and

(See figure on next page.)

Fig. 4 Overexpression of CDH4 improved the proliferation, stemness and motility of OSCC. CDH4 expression was effectively increased by pcDNA3.1-FLAG-CDH4 plasmid as measured by western blot **A**. The growth of HN30 cells was measured by CCK-8 assay **B**. The colony formation assay showed that the proliferation of HN30 cells was increased after CDH4 up-regulation **C**. The number of colonies was counted **D**. The picture shows the cell sphere formation in different groups under a 40X microscope **E**, and the number of spheres was increased in the CDH4-overexpression group compared with the vector group **F**. For the wound-heal assay, the representative images show the distances of cells passing through the scratch within a period of time for HN30 cells **G** under a 40X microscope field of view. The mobility rate of cells was measured for HN30 cells **H**. In the transwell migration assay, representative images show the cells transfected that passed through the upper chamber of the transwell without (upper panel) Matrigel coating for HN30 cells **I**. The number of cells that passed through the filters was counted for HN30 cells **J**. In the transwell invasion assay, representative images show the cells transfected that passed through the upper chamber of the transwell with (upper panel) Matrigel coating for HN30 cells **K**. The number of cells that passed through the filters was counted for HN30 cells **L**. The numbers of migrating cells were counted from at least five randomly selected fields of view under a microscope at 100X magnification. These experiments were repeated three times. (* indicates $P < 0.05$, **indicates $P < 0.01$, ***indicates $P < 0.001$, ****indicates $P < 0.0001$, Values are presented as means \pm standard error.)

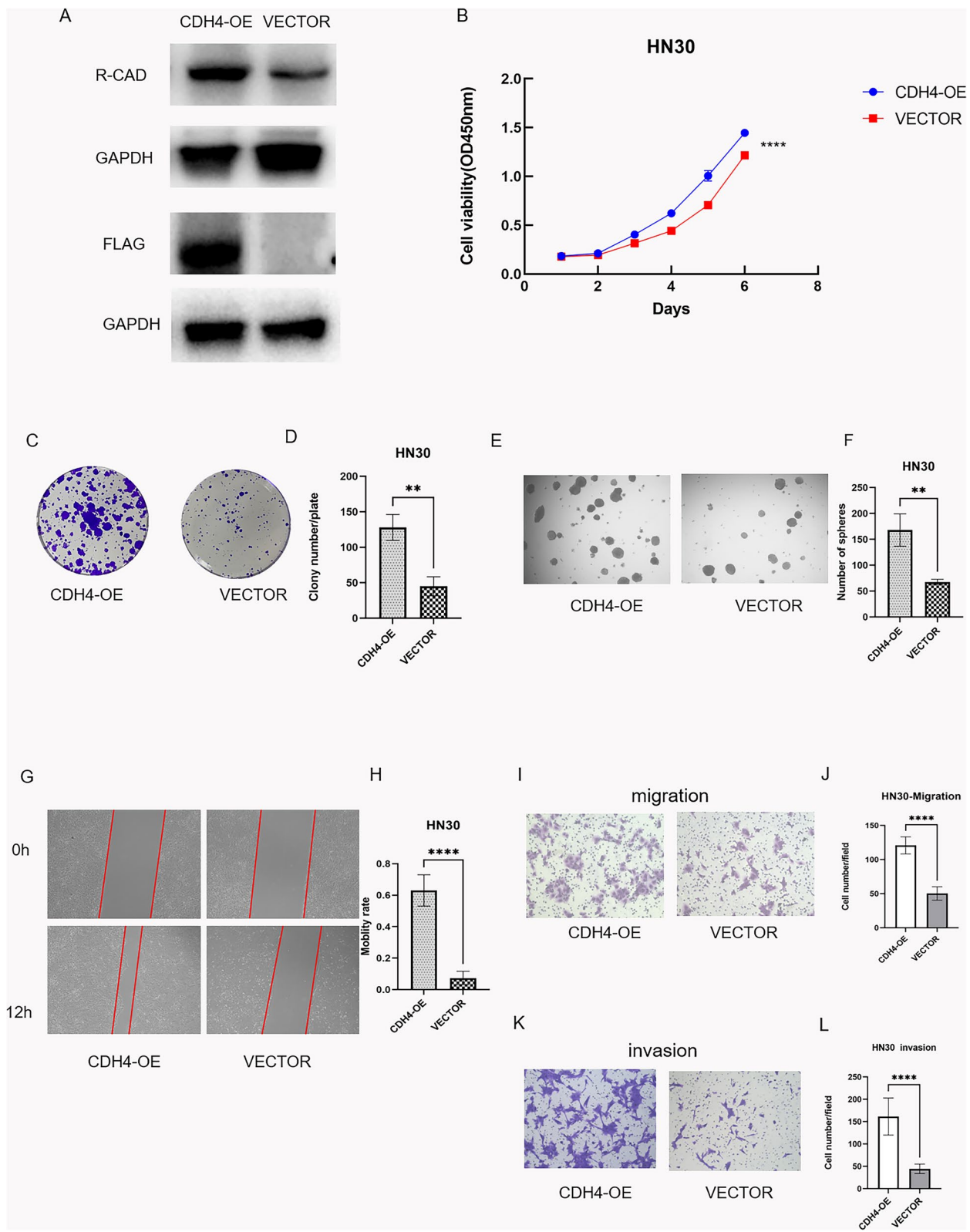


Fig. 4 (See legend on previous page.)

plate colony formation experiments confirmed that cell proliferation in the siRNA-1 and siRNA-2 groups was lower than that in the NC group in HN30 cells (Fig. 2G,I) and SCC9 cells (Fig. 2H,J). Cell spheroidization experiments showed that the self-renewal of cells was decreased in the siRNA-1 and siRNA-2 groups compared with the NC group in HN30 cells (Fig. 2K-L). Downregulation of the CDH4 gene inhibits the proliferation and self-renewal of OSCC cells in vitro.

Downregulation of CDH4 expression suppresses OSCC migration and invasion in vitro

We found that cell mobility and invasion ability were weakened after siRNA downregulated the expression of CDH4. In the transwell migration assay and transwell invasion assay, the numbers of cells that passed through the monolayers of the upper panel of transwells without Matrigel and transwells with Matrigel in the siRNA-1 and siRNA-2 groups were lower than that in the NC group in HN30 cells (Fig. 3A-C) and SCC9 cells (Fig. 3D-F). Furthermore, wound healing assays showed that the mobility of cells in the siRNA-1 and siRNA-2 groups was slower than that in the NC group in HN30 cells (Fig. 3G-H) and SCC9 cells (Fig. 3I-J). Downregulation of the CDH4 gene inhibits the mobility of OSCC cells in vitro.

Overexpression of CDH4 improved the proliferation, mobility and stemness of OSCC cells in vitro

After the functional experiment of CDH4-down-regulation, we up-regulated the expression of CDH4 and studied the changes of cell functions. Changes in cell proliferation ability and mobility were observed after up-regulated the expression of CDH4. The expression of CDH4 was up-regulation in CDH4-overexpression group than vector group (Fig. 4A). CCK-8 assays and plate colony formation experiments confirmed that cell proliferation in the CDH4-overexpression group was higher compared with the vector group in HN30 cells (Fig. 4B-D). Cell spheroidization experiments showed that the self-renewal of cells was increased in the CDH4-overexpression groups compared with the vector group in HN30 cells (Fig. 4E-F). In wound healing assays showed that the mobility of cells in the CDH4-overexpression groups was faster than that in the vector group in HN30 cells (Fig. 4G-H). Furthermore, in the transwell migration assay and transwell invasion assay, the numbers of cells that passed through the

monolayers of the upper panel of transwells without and with Matrigel in the CDH4-overexpression groups were more than that in the vector group in HN30 cells (Fig. 4I-L). Up-regulation of the CDH4 gene improves the proliferation, self-renewal and mobility of OSCC cells in vitro.

Through the above cytological function experiments, we found that CDH4 gene can promote cell proliferation, self-renewal, invasion and migration. We began to observe the reason why CDH4 gene can change the cell function, and whether the change of cell proliferation is related to the occurrence of ferroptosis.

CDH4 can resist the sensitivity of OSCC cells to ferroptosis

The cell staining assay showed that the mortality rate of HN30 cells is dramatically increased by downregulation of CDH4 and decreased by up-regulation of CDH4 (Fig. 5A-D). Through western blot experiments, we found that compared with the NC control group, the GPX4 in siRNA-1 and siRNA-2 groups down-regulated by CDH4 decreased (Fig. 5E). Compared with vector group, the expression of GPX4 in CDH4-overexpression group was higher (Fig. 5F). Ferroptosis is due to the inactivation of antioxidant system in cells, which leads to the accumulation of lipid hydroperoxide in cells and eventually leads to cell death [51]. The system xc – glutathione (GSH)-GPX4-dependent antioxidant defense is the most important [52]. GPX4 is an antioxidant enzyme. When ferroptosis in GPX4 path, reduced GSH will become GSSG with the help of GPX4 [53]. After discovering the change of GPX4, we detected the change of GSH/GSSG. Compared with NC group, GSH in siRNA-1 and siRNA-2 groups decreased, GSSG increased and GSH/GSSG ratio decreased (Fig. 5G). Compared with vector group, GSH increased, GSSG decreased and GSH/GSSG ratio increased in CDH4-overexpression group (Fig. 5H). When oxygen free radicals react with unsaturated fatty acids of lipids to produce lipid peroxide as a by-product, we detect the level of lipid oxidation by detecting the level of MDA. The MDA experiment proved that the MDA produced by cells increased after the down-regulation of CDH4 expression, and decreased after the up-regulation of CDH4 expression (Fig. 5I-J). The above experiments confirmed that CDH4 can resist the sensitivity of cells to ferroptosis and suggest that the effect of CDH4 on cell proliferation may be due to its resistance to ferroptosis of cells.

(See figure on next page.)

Fig. 5 CDH4 can reduce the sensitivity of OSCC cells to ferroptosis. In the representative images, live cells fluoresced green (Calcein/AM) and dead cells fluoresced red (PI) **A, C**. The images include at least five randomly selected fields of view under a 400X laser confocal microscope. The statistical graph shows the percentage of dead cells **B, D**. The western blot experiment showed the expression of GPX4 in the CDH4 down-regulation experiment and CDH4 up-regulation experiment **E-F**. The expression of GSH, GSSG and the ratio of GSH/GSSG in the CDH4 down-regulation experiment and CDH4 up-regulation experiment **G-H**. The MDA in the CDH4 down-regulation experiment and CDH4 up-regulation experiment (Fig. I-J). (* indicates $P < 0.05$, ** indicates $P < 0.01$, *** indicates $P < 0.001$, **** indicates $P < 0.0001$, and Values are presented as means \pm standard error.)

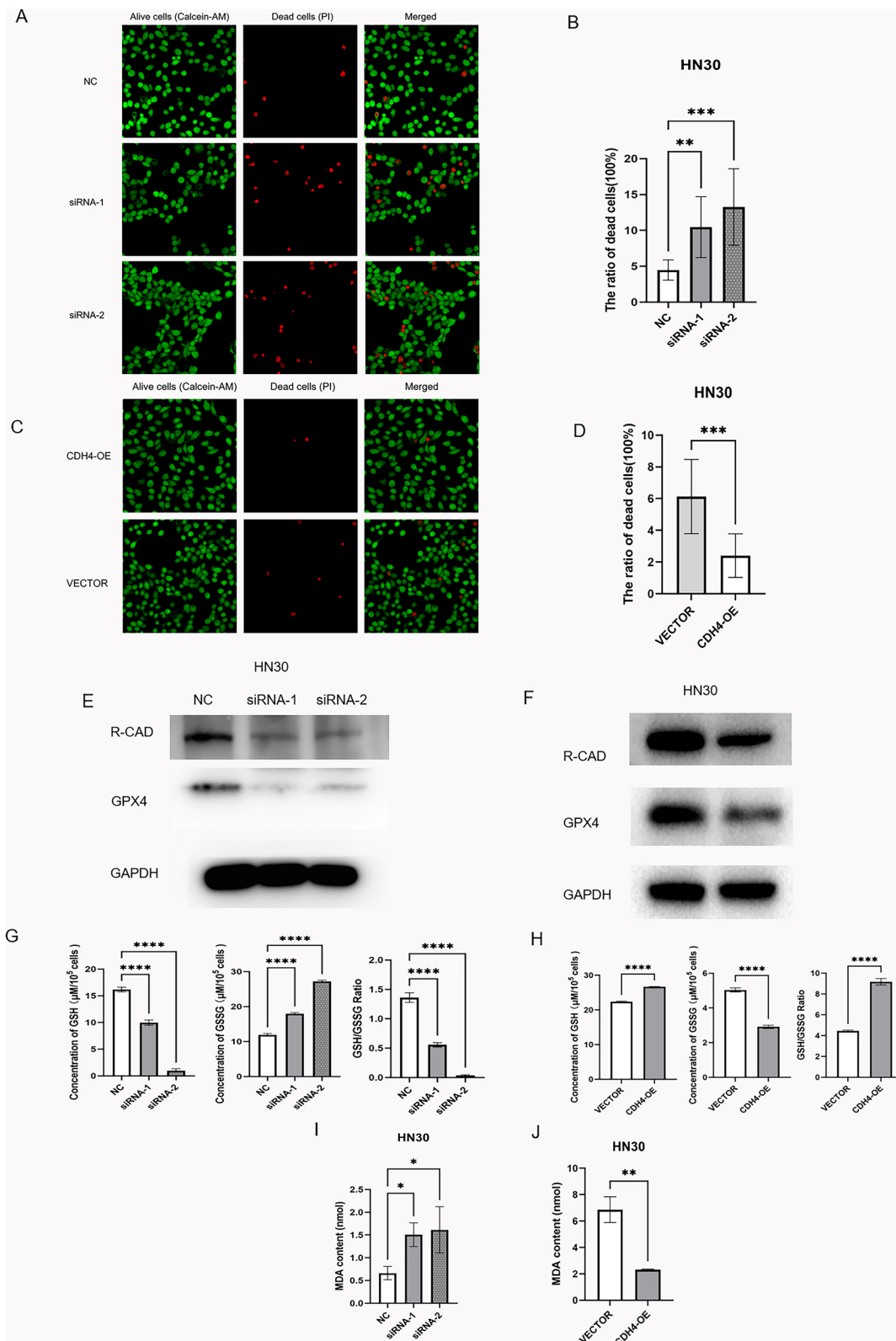


Fig. 5 (See legend on previous page.)

CDH4-related pathway analysis

In OSCC, CDH4 is considered to promote the proliferation and metastasis of cells and play a role in the development of tumors. We used bioinformatics to analyze the database samples, hoping to find the related genes and pathways to explain the mechanism of CDH4. In order to explore suitable pathways, we chose to start with HNSCC for a larger sample size, and after verifying the corresponding pathways, we analyzed the correlation between the related genes of these pathways and CDH4 in OSCC. Moreover, we also analyzed the correlation between CDH4 and key genes of ferroptosis to find out the possible mechanism of CDH4. We found the top ten related pathways that correlated with CDH4 by GSEA in the Hallmark gene set in HNSCC (Fig. 6A). We selected three pathways that are most likely to be related to the previous experiments, such as the EMT pathway (Fig. 6B), fatty acid metabolism pathway (Fig. 6C) and peroxisome pathway (Fig. 6D). The EMT pathway was significantly positively correlated with CDH4 in OSCC. It had 13 genes positively correlated with CDH4 in EMT (Fig. 6E). The fatty acid metabolism pathway and peroxisome pathway were found many genes negatively correlated with CDH4 (Fig. 6F-G). CDH4 gene is also related to many key genes of ferroptosis in OSCC (Fig. 6H-J). These results indicated that CDH4 protects cell proliferation by resisting ferroptosis, while the promotion of cell mobility by CDH4 may be related to EMT pathway.

Discussion

CDH4 encodes R-cadherin, which is a member of the cadherin family. The function of R-cad in tumors is controversial, and its role in OSCC is unknown. Some studies have shown that CDH4 is a tumor suppressor in nasopharyngeal carcinoma, gastrointestinal tumors, mammary tumors and lung cancer [18–22]. In another previous study, CDH4 was shown to be a gene that promotes cancer [23–27]. R-cadherin expression has been found in rhabdomyosarcomas and is absent in normal myoblasts [24]. In renal cell carcinoma, the expression of CDH4 is higher than that in normal kidney tissue [25]. By analyzing the TCGA database, the results show that CDH4 is more highly expressed in cancer tissue than in normal tissue in HNSCC and OSCC. Clinical OSCC samples also confirmed that CDH4 is highly expressed in cancer tissue. R-cadherin improves the motility of cells

via GTPase activity in cervical cancer [26]. Our study also confirmed that CDH4 promoted the cells motility and proliferation in OSCC.

In osteosarcoma, CDH4 was shown to activate c-Jun via the JNK pathway and improve self-renewal ability to promote tumorigenesis and metastasis [27]. Tumor cells self-renewal ability play an important role in tumor survival, proliferation, metastasis and recurrence. Postoperative recurrence is an obstacle in the treatment of OSCC [54, 55]. We had the same finding about CDH4 in OSCC. CDH4 enhanced the self-renewal ability of tumor cells in OSCC.

Through GSEA of the Hallmark gene set, CDH4 was found positively correlated with multiple tumor-related pathways. In particular, it has a high correlation with the EMT pathway. EMT is a key pathway in tumor metastasis and recurrence. The sample size of OSCC is over 300. For the large sample data over 300, the samples with R value of correlation analysis above 0.1 and $P < 0.05$ are considered to have significant correlation. EMT is a classical and important pathway for cadherin to promote cell invasion and metastasis, and it is studied daily in tumors. Correlation analysis showed that 13 genes in EMT pathway were positively correlated with CDH4. EMT occurs because the expression of E-cadherin (CDH1 coding), which expresses epithelial characteristics, is suppressed, and the expression of N-cadherin (CDH2/CDH12 coding), which expresses mesenchymal characteristics, is increased [56]. Cells change from epithelial characteristics to mesenchymal characteristics, making it easier for cells to move [57]. The occurrence of EMT will cause the invasion and metastasis of tumor cells. EMT correlation analysis showed that CDH4 was positively correlated with FOXC2 and CDH2 gene. FOXC2 can inhibit the expression of E-cadherin, and N-cadherin has been proved to promote tumor in OSCC [58, 59].

After analyzing the genes related to CDH4, we found that except the above two genes, the other genes PLDO3, FSTL3, COLGALT1, FN1, PMEPA1, LGALS1, COL4A2, SERPINH1 and SPOCK1 were all found to promote the occurrence and development of different tumors [60–68]. Because there is a positive correlation between CDH4 and these genes, we think that CDH4 may play a positive role in EMT, which affects the movement and invasion of tumor cells through EMT pathway.

(See figure on next page.)

Fig. 6 GSEA of CDH4 in the Hallmark gene set. Top ten related CDH4 pathways by GSEA hallmark enrichment analysis in HNSCC **A**. The EMT pathway is positively correlated with CDH4, fatty acid metabolism pathway and peroxisome pathway is negatively correlated with CDH4 in HNSCC **B-D**. Correlation analysis showed that EMT pathway gene was related to CDH4 in OSCC **E**. Correlation analysis showed that fatty acid metabolism pathway genes were related to CDH4 in OSCC **F**. Correlation analysis showed that peroxisome pathway genes were related to CDH4 in OSCC **G**. Correlation analysis showed that ferroptosis related genes were related to CDH4 in OSCC **H-J** (* indicates $P < 0.05$, ** indicates $P < 0.01$, *** indicates $P < 0.001$, **** indicates $P < 0.0001$, and Values are presented as means \pm standard error.)

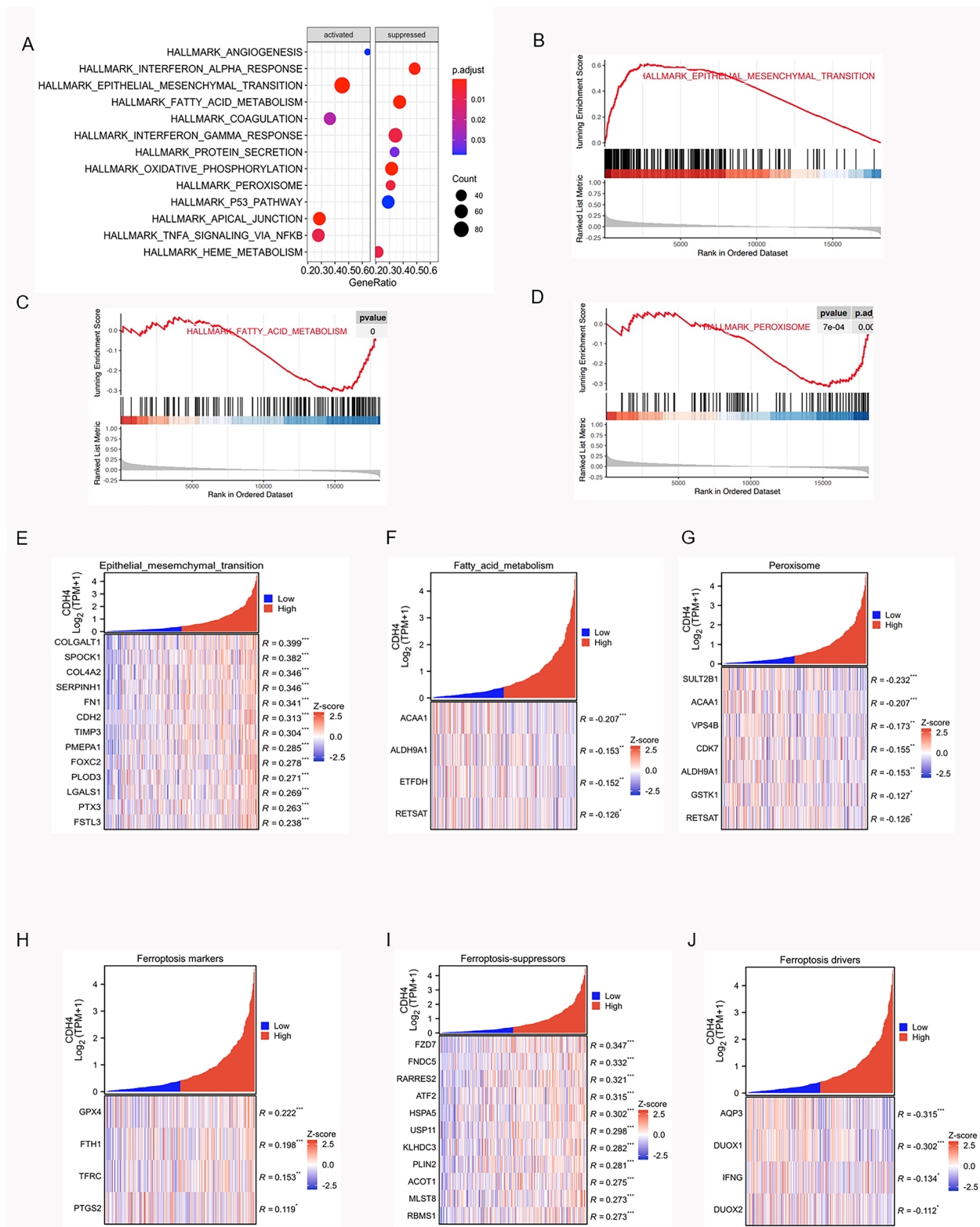


Fig. 6 (See legend on previous page.)

Some studies point out that there is a relationship between cadherins and ferroptosis. E-cadherin activates the Merlin and Hippo signaling pathways to suppress ferroptosis. Cancer cells with epithelial properties are less sensitive to ferroptosis than those with mesenchymal properties [69]. VE-cadherin can resist the destruction of blood–brain barrier cells caused by iron metabolism disorder [70].

According to the results of previous experiments, we think that the change of cell proliferation ability caused by CDH4 is because it resisted the sensitivity of cells to ferroptosis. Ferroptosis is caused by iron metabolism abnormality and two redox systems (lipid peroxidation and thiols) abnormality are the causes of iron-dependent ROS accumulation in cells [33]. Experiments confirmed that the raising consumption of GSH and GPX4 and the increase of intracellular lipid peroxidation occurred after the decreasing of CDH4 in OSCC. We used enrichment analysis show two correlation pathways: fatty acid metabolism pathway peroxisome pathway. We verified that the related genes of these two pathways of CDH4 were negatively correlated in OSCC. We analyzed the correlation between CDH4 and ferroptosis marker genes, ferroptosis suppressor genes and ferroptosis driver genes in OSCC. Data shows that half of marker genes (GPX4, FTH1, TFRC, PTGS2) of ferroptosis were correlated with CDH4, and the CDH4 was positively correlated with the genes (FZD7, FIDC5, RARRES2, ATF2, HSPA5, USP11, KLHDC3, PLIN2, ACOT1, MLST8, RBMS1) that inhibit ferroptosis and negatively correlated with the genes (AQP3, NOX5, DUOX1, DUOX2) that promote ferroptosis.

Conclusions

In summary, CDH4 effectively promotes the proliferation, invasion and metastasis of OSCC cells. It may enhance EMT pathway and reduce the sensitivity of OSCC cells to ferroptosis. CDH4 is a therapeutic target in OSCC.

Supplementary Information

The online version contains supplementary material available at <https://doi.org/10.1186/s12903-023-03046-3>.

Additional file 1.

Acknowledgements

Not applicable

Authors' contributions

All authors read and approved the final manuscript. All authors have made a sufficient contribution to the work. Concept and design: YGL and DLZ. Experiments and procedures: JX, TL, LCD. Data analysis: JX, TL, YGL, DLZ. Writing and editing the article: XJ, LCD, DLZ, YGL.

Funding

This work was supported by the National Natural Science Foundation of China [grant number: 82272868 and 82173180]; and the Innovation Foundation of Department of Science and Technology of Fujian (grant number: 2017Y9096), Fujian Medical Innovation Grant [grant number: 2018-CXB-13]; and the research grant of Fujian Provincial Education Department [grant number: JT180206]. The funding bodies had no role in the design of the study and collection, analysis, and interpretation of data and in writing the manuscript.

Availability of data and materials

All data generated or analyzed during this study are included in this published article.

Declarations

Ethics approval and consent to participate

The study was approved by the Ethics Committee of the Fujian Medical University, ethical number 2021-FMUS-024. Informed consent was obtained by all participants. The study was performed in accordance with the provisions of the Declaration of Helsinki (as revised in Edinburgh 2000).

Consent for publication

Not applicable.

Competing interests

The authors declare no potential competing interests.

Received: 6 January 2023 Accepted: 15 May 2023

Published online: 27 May 2023

References

- Kemler R. Classical cadherins. *Semin Cell Biol.* 1992;3(3):149–55. [https://doi.org/10.1016/s1043-4682\(10\)80011-x](https://doi.org/10.1016/s1043-4682(10)80011-x). (PMID: 1623204).
- Takeichi M. Cadherins: a molecular family important in selective cell-cell adhesion. *Annu Rev Biochem.* 1990;59:237–52. <https://doi.org/10.1146/annurev.bi.59.070190.001321>.
- Conacci-Sorrell M, Zhurinsky J, Ben-Ze'ev A. The cadherin-catenin adhesion system in signaling and cancer. *J Clin Invest.* 2002;109(8):987–91. <https://doi.org/10.1172/JCI15429>. PMID: 11956233; PMCID: PMC150951.
- Goodsell DS. The molecular perspective: cadherin. *Stem Cells.* 2002;20(6):583–4. <https://doi.org/10.1634/stemcells.20-6-583>.
- Kaszak I, Witkowska-Piłaszewicz O, Niewiadomska Z, Dworecka-Kaszak B, Ngosa Toka F, Jurka P. Role of cadherins in cancer—a review. *Int J Mol Sci.* 2020;21(20):7624. <https://doi.org/10.3390/ijms21207624>. PMID: 33076339; PMCID: PMC7589192.
- Ebnet K, Kummer D, Steinbacher T, Singh A, Nakayama M, Matis M. Regulation of cell polarity by cell adhesion receptors. *Semin Cell Dev Biol.* 2018;81:2–12. <https://doi.org/10.1016/j.semdb.2017.07.032>. (Epub 2017 Jul 22).
- Shahbazi MN, Perez-Moreno M. Connections between cadherin-catenin proteins, spindle misorientation, and cancer. *Tissue Barriers.* 2015;3(3).
- Casal JI, Bartolomé RA. Beyond N-cadherin, relevance of cadherins 5, 6 and 17 in cancer progression and metastasis. *Int J Mol Sci.* 2019;20(13):3373. <https://doi.org/10.3390/ijms20133373>.
- Li Y, Lv Z, Zhang S, et al. Genetic fate mapping of transient cell fate reveals N-cadherin activity and function in tumor metastasis. *Cell.* 2020;54(5):593–607.e5. <https://doi.org/10.1016/j.devcel.2020.06.021>. (Epub 2020 Jul 14).
- Mendonça AM, Na TY, Gumbiner BM. E-cadherin in contact inhibition and cancer. *Oncogene.* 2018;37(35):4769–80. <https://doi.org/10.1038/s41388-018-0304-2>. (Epub 2018 May 21).
- Hugo HJ, Gunasinghe NPAD, Hollier BG, et al. Epithelial requirement for in vitro proliferation and xenograft growth and metastasis of MDA-MB-468 human breast cancer cells: oncogenic rather than

- tumor-suppressive role of E-cadherin. *Breast Cancer Res.* 2017;19(1):86. <https://doi.org/10.1186/s13058-017-0880-z>.
12. Delgado-Bellido D, Serrano-Saenz S, Fernández-Cortés M, et al. Vasculogenic mimicry signaling revisited: focus on non-vascular VE-cadherin. *Mol Cancer.* 2017;16(1):65. <https://doi.org/10.1186/s12943-017-0631-x>.
 13. Babb SG, Kotradi SM, Shah B, et al. Zebrafish R-cadherin (Cdh4) controls visual system development and differentiation. *Dev Dyn.* 2005;233(3):930–45. <https://doi.org/10.1002/dvdy.20431>.
 14. Rosenberg P, Esni F, Sjödin A, et al. A potential role of R-cadherin in striated muscle formation. *Dev Biol.* 1997;187(1):55–70. <https://doi.org/10.1006/dbio.1997.8602>.
 15. Dahl U, Sjödin A, Larue L, et al. Genetic dissection of cadherin function during nephrogenesis. *Mol Cell Biol.* 2002;22(5):1474–87. <https://doi.org/10.1128/MCB.22.5.1474-1487.2002>.
 16. Wiszniewski W, Gawlinski P, Gambin T, et al. Comprehensive genomic analysis of patients with disorders of cerebral cortical development. *Eur J Hum Genet.* 2018;26(8):1121–31. <https://doi.org/10.1038/s41431-018-0137-z>. (Epub 2018 Apr 30).
 17. Lin J, Wang C, Redies C. Restricted expression of classic cadherins in the spinal cord of the chicken embryo. *Front Neuroanat.* 2014;3(8):18. <https://doi.org/10.3389/fnana.2014.00018>.
 18. Du C, Huang T, Sun D, et al. CDH4 as a novel putative tumor suppressor gene epigenetically silenced by promoter hypermethylation in nasopharyngeal carcinoma. *Cancer Lett.* 2011;309(1):54–61. <https://doi.org/10.1016/j.canlet.2011.05.016>. (Epub 2011 Jun 12).
 19. Xie J, Feng Y, Lin T, Huang XY, et al. CDH4 suppresses the progression of salivary adenoid cystic carcinoma via E-cadherin co-expression. *Oncotarget.* 2016;7(50):82961–71. <https://doi.org/10.18632/oncotarget.12821>.
 20. Li Z, Su D, Ying L, et al. Study on expression of CDH4 in lung cancer. *World J Surg Oncol.* 2017;15(1):26. <https://doi.org/10.1186/s12957-016-1083-2>.
 21. Agiostratidou G, Li M, Suyama K, et al. Loss of retinal cadherin facilitates mammary tumor progression and metastasis. *Cancer Res.* 2009;69(12):5030–8. <https://doi.org/10.1158/0008-5472.CAN-08-4007>. (Epub 2009 Jun 2).
 22. Miotto E, Sabbioni S, Veronese A, et al. Frequent aberrant methylation of the CDH4 gene promoter in human colorectal and gastric cancer. *Cancer Res.* 2004;64(22):8156–9. <https://doi.org/10.1158/0008-5472.CAN-04-3000>.
 23. Ceresa D, Alessandrini F, Bosio L, et al. Cdh4 Down-Regulation Impairs in Vivo Infiltration and Malignancy in Patients Derived Glioblastoma Cells. *Int J Mol Sci.* 2019;20(16):4028. <https://doi.org/10.3390/ijms20164028>.
 24. Kucharczak J, Charrasse S, Comunale F, et al. R-Cadherin expression inhibits myogenesis and induces myoblast transformation via Rac1 GTPase. *Cancer Res.* 2008;68(16):6559–68. <https://doi.org/10.1158/0008-5472.CAN-08-0196>.
 25. Zhou X, Huang H, Cui W, et al. Expression and Prognostic Significance of Cadherin 4 (CDH4) in Renal Cell Carcinoma. *Med Sci Monit.* 2020;26:e922836.
 26. Johnson E, Theisen CS, Johnson KR, et al. R-cadherin influences cell motility via Rho family GTPases. *J Biol Chem.* 2004 Jul 23;279(30):31041–9. doi: <https://doi.org/10.1074/jbc.M400024200>. Epub 2004 May 13. Erratum in: *J Biol Chem.* 2004 Oct 15;279(42):44230.
 27. Tang Q, Lu J, Zou C, et al. CDH4 is a novel determinant of osteosarcoma tumorigenesis and metastasis. *Oncogene.* 2018;37(27):3617–30. <https://doi.org/10.1038/s41388-018-0231-2>. (Epub 2018 Apr 3).
 28. Dixon SJ, Lemberg KM, Lamprecht MR, et al. Ferroptosis: an iron-dependent form of nonapoptotic cell death. *Cell.* 2012;149(5):1060–72. <https://doi.org/10.1016/j.cell.2012.03.042>.
 29. Gan B. Mitochondrial regulation of ferroptosis. *J Cell Biol.* 2021;220(9):e202105043.
 30. Zhao L, Zhou X, Xie F, Zhang L, Yan H, Huang J, Zhang C, Zhou F, Chen J, Zhang L. Ferroptosis in cancer and cancer immunotherapy. *Cancer Commun (Lond).* 2022;42(2):88–116. <https://doi.org/10.1002/cac2.12250>.
 31. Lei G, Zhuang L, Gan B. Targeting ferroptosis as a vulnerability in cancer. *Nat Rev Cancer.* 2022;22(7):381–96. <https://doi.org/10.1038/s41568-022-00459-0>. (Epub 2022 Mar 25).
 32. Hassannia B, Vandenabeele P, Vanden BT. Targeting ferroptosis to iron out cancer. *Cancer Cell.* 2019;35(6):830–49. <https://doi.org/10.1016/j.ccell.2019.04.002>. (Epub 2019 May 16).
 33. Mou Y, Wang J, Wu J, et al. Ferroptosis, a new form of cell death: opportunities and challenges in cancer. *J Hematol Oncol.* 2019;12(1):34. <https://doi.org/10.1186/s13045-019-0720-y>.
 34. Yu H, Guo P, Xie X, et al. Ferroptosis, a new form of cell death, and its relationships with tumorous diseases. *J Cell Mol Med.* 2017;21(4):648–57. <https://doi.org/10.1111/jcmm.13008>. (Epub 2016 Nov 10).
 35. Zhang C, Liu X, Jin S, Chen Y, Guo R. Ferroptosis in cancer therapy: a novel approach to reversing drug resistance. *Mol Cancer.* 2022;21(1):47. <https://doi.org/10.1186/s12943-022-01530-y>.
 36. Sung H, Ferlay J, Siegel RL, et al. Global Cancer Statistics 2020: GLOBOCAN Estimates of Incidence and Mortality Worldwide for 36 Cancers in 185 Countries. *CA Cancer J Clin.* 2021;71(3):209–49. <https://doi.org/10.3322/caac.21660>. (Epub 2021 Feb 4).
 37. Siegel RL, Miller KD, Fuchs HE, et al. Cancer Statistics, 2021. *CA Cancer J Clin.* 2021;71(1):7–33. doi: <https://doi.org/10.3322/caac.21654>. Epub 2021 Jan 12. Erratum in: *CA Cancer J Clin.* 2021;71(4):359.
 38. Taghavi N, Yazdi I. Prognostic factors of survival rate in oral squamous cell carcinoma: clinical, histologic, genetic and molecular concepts. *Arch Iran Med.* 2015;18(5):314–9.
 39. Ford PJ, Rich AM. Tobacco use and oral health. *Addiction.* 2021;116(12):3531–40. <https://doi.org/10.1111/add.15513>. (Epub 2021 Apr 25).
 40. Argiris A, Karamouzis MV, Raben D, et al. Head and neck cancer. *Lancet.* 2008;371(9625):1695–709. [https://doi.org/10.1016/S0140-6736\(08\)60728-X](https://doi.org/10.1016/S0140-6736(08)60728-X).
 41. von Witzleben A, Wang C, Laban S, Savelieva N, Ottensmeier CH. HNSCC: tumour antigens and their targeting by immunotherapy. *Cells.* 2020;9(9):2103. <https://doi.org/10.3390/cells9092103>.
 42. Lindemann A, Takahashi H, Patel AA, et al. Targeting the DNA damage response in OSCC with TP53 mutations. *J Dent Res.* 2018;97(6):635–44. <https://doi.org/10.1177/0022034518759068>. (Epub 2018 Feb 28).
 43. Huang WC, Jang TH, Tung SL, et al. A novel miR-365-3p/EHF/keratin 16 axis promotes oral squamous cell carcinoma metastasis, cancer stemness and drug resistance via enhancing β 5-integrin/c-met signaling pathway. *J Exp Clin Cancer Res.* 2019;38(1):89. <https://doi.org/10.1186/s13046-019-1091-5>.
 44. Polizzi A, Santonocito S, Lo Giudice A, Alibrandi A, De Pasquale R, Isola G. Analysis of the response to two pharmacological protocols in patients with oral lichen planus: A randomized clinical trial. *Oral Dis.* 2023;29(2):755–63. <https://doi.org/10.1111/odi.13960>. (Epub 2021 Jul 29 PMID: 34252252).
 45. Lodi G, Franchini R, Warnakulasuriya S, Varoni EM, Sardella A, Kerr AR, Carrassi A, MacDonald LC, Worthington HV. Interventions for treating oral leukoplakia to prevent oral cancer. *Cochrane Database Syst Rev.* 2016;7(7):CD001829.
 46. Isola G, Matarese M, Ramaglia L, Iorio-Siciliano V, Cordasco G, Matarese G. Efficacy of a drug composed of herbal extracts on postoperative discomfort after surgical removal of impacted mandibular third molar: a randomized, triple-blind, controlled clinical trial. *Clin Oral Investig.* 2019;23(5):2443–53. <https://doi.org/10.1007/s00784-018-2690-9>. (Epub 2018 Oct 11 PMID: 30311061).
 47. Li H, Zhang Y, Xu M, Yang D. Current trends of targeted therapy for oral squamous cell carcinoma. *J Cancer Res Clin Oncol.* 2022;148(9):2169–86. <https://doi.org/10.1007/s00432-022-04028-8>. (Epub 2022 May 2 PMID: 35501496).
 48. Sinto MS, Thomas S, Kannan S. Combinatorial treatment with Gefitinib and Bay11-7085 sensitizes primary Gefitinib-resistant OSCC cells by influencing the EGFR- NF κ B signaling axis. *Med Oncol.* 2021;38(9):110. <https://doi.org/10.1007/s12032-021-01557-z>.
 49. Ohnishi Y, Yasui H, Nozaki M, et al. Molecularly-targeted therapy for the oral cancer stem cells. *Jpn Dent Sci Rev.* 2018;54(2):88–103. <https://doi.org/10.1016/j.jdsr.2017.11.001>. (Epub 2017 Dec 16).
 50. Wang J, Chen X, Tian Y, et al. Six-gene signature for predicting survival in patients with head and neck squamous cell carcinoma. *Aging (Albany NY).* 2020;12(1):767–83. <https://doi.org/10.18632/aging.102655>.
 51. Kajarabille N, Latunde-Dada GO. Programmed cell-death by ferroptosis: antioxidants as mitigators. *Int J Mol Sci.* 2019;20(19):4968. <https://doi.org/10.3390/ijms20194968>.

52. Dahlmanns M, Yakubov E, Dahlmanns JK. Genetic profiles of ferroptosis in malignant brain tumors and off-target effects of ferroptosis induction. *Front Oncol.* 2021;11:783067.
53. Ursini F, Maiorino M. Lipid peroxidation and ferroptosis: The role of GSH and GPx4. *Free Radic Biol Med.* 2020;20(152):175–85. <https://doi.org/10.1016/j.freeradbiomed.2020.02.027>. (Epub 2020 Mar 9).
54. Gleber-Netto FO, Braakhuis BJ, Triantafyllou A, Takes RP, Kelner N, Rodrigo JP, Strojjan P, Vander Poorten V, Rapidis AD, Rinaldo A, Brakenhoff RH, Ferlito A, Kowalski LP. Molecular events in relapsed oral squamous cell carcinoma: recurrence vs. secondary primary tumor. *Oral Oncol.* 2015;51(8):738–44.
55. Liu CH, Chen HJ, Wang PC, Chen HS, Chang YL. Patterns of recurrence and second primary tumors in oral squamous cell carcinoma treated with surgery alone. *Kaohsiung J Med Sci.* 2013;29(10):554–9. <https://doi.org/10.1016/j.kjms.2013.03.001>. (Epub 2013 Jun 7 PMID: 24099110).
56. Pastushenko I, Blanpain C. EMT Transition States during tumor progression and metastasis. *Trends Cell Biol.* 2019;29(3):212–26. <https://doi.org/10.1016/j.tcb.2018.12.001>. (Epub 2018 Dec 26).
57. Brabletz S, Schuhwerk H, Brabletz T, Stemmler MP. Dynamic EMT: a multi-tool for tumor progression. *EMBO J.* 2021;40(18):e108647.
58. Recouvreur MS, Miao J, Gozo MC, Wu J, Walts AE, Karlan BY, Orsulic S. FOXC2 promotes vasculogenic mimicry in ovarian cancer. *Cancers (Basel).* 2022;14(19):4851. <https://doi.org/10.3390/cancers14194851>.
59. Loh CY, Chai JY, Tang TF, Wong WF, Sethi G, Shanmugam MK, Chong PP, Looi CY. The E-Cadherin and N-Cadherin switch in epithelial-to-mesenchymal transition: signaling, therapeutic implications, and challenges. *Cells.* 2019;8(10):1118. <https://doi.org/10.3390/cells8101118>.
60. Qi Y, Xu R. Roles of PLODs in collagen synthesis and cancer progression. *Front Cell Dev Biol.* 2018;28(6):66. <https://doi.org/10.3389/fcell.2018.00066>.
61. Tian S, Xu X, Yang X, Fan L, Jiao Y, Zheng M, Zhang S. Roles of follistatin-like protein 3 in human non-tumor pathophysiology and cancers. *Front Cell Dev Biol.* 2022;10:953551.
62. Liu S, Yu Y, Wang Y, Zhu B, Han B. COLGALT1 is a potential biomarker for predicting prognosis and immune responses for kidney renal clear cell carcinoma and its mechanisms of ceRNA networks. *Eur J Med Res.* 2022;27(1):122. <https://doi.org/10.1186/s40001-022-00745-5>.
63. Li J, Chen C, Chen B, Guo T. High FN1 expression correlates with gastric cancer progression. *Pathol Res Pract.* 2022;239:154179.
64. Qiu D, Hu J, Hu J, Yu A, Othmane B, He T, Ding J, Cheng X, Ren W, Tan X, Yu Q, Chen J, Zu X. PMEPA1 is a prognostic biomarker that correlates with cell malignancy and the tumor microenvironment in bladder cancer. *Front Immunol.* 2021;12:705086.
65. Sun H, Zhang H, Yan Y, Li Y, Che G, Zhou C, Nicot C, Ma H. NCAPG promotes the oncogenesis and progression of non-small cell lung cancer cells through upregulating LGALS1 expression. *Mol Cancer.* 2022;21(1):55. <https://doi.org/10.1186/s12943-022-01533-9>. Erratum in: *Mol Cancer.* 2022 Dec 14;21(1):221.
66. JingSong H, Hong G, Yang J, Duo Z, Li F, WeiCai C, XueYing L, YouSheng M, YiWen O, Yue P, Zou C. siRNA-mediated suppression of collagen type iv alpha 2 (COL4A2) mRNA inhibits triple-negative breast cancer cell proliferation and migration. *Oncotarget.* 2017;8(2):2585–93. <https://doi.org/10.18632/oncotarget.13716>.
67. Tian S, Peng P, Li J, Deng H, Zhan N, Zeng Z, Dong W. SERPINH1 regulates EMT and gastric cancer metastasis via the Wnt/ β -catenin signaling pathway. *Aging (Albany NY).* 2020;12(4):3574–93. <https://doi.org/10.18632/aging.102831>. (Epub 2020 Feb 24).
68. Sun LR, Li SY, Guo QS, Zhou W, Zhang HM. SPOCK1 involvement in epithelial-to-mesenchymal transition: a new target in cancer therapy? *Cancer Manag Res.* 2020;18(12):3561–9. <https://doi.org/10.2147/CMAR.S249754>.
69. Lee J, You JH, Kim MS, et al. Epigenetic reprogramming of epithelial-mesenchymal transition promotes ferroptosis of head and neck cancer. *Redox Biol.* 2020 Oct; 37:101697. doi: <https://doi.org/10.1016/j.redox.2020.101697>. Epub 2020 Aug 28.
70. Rand D, Ravid O, Atrakchi D, et al. Endothelial iron homeostasis regulates blood-brain barrier integrity via the HIF2 α -Ve-Cadherin pathway. *Pharmaceutics.* 2021;13(3):311. <https://doi.org/10.3390/pharmaceutics13030311>.

Publisher's Note

Springer Nature remains neutral with regard to jurisdictional claims in published maps and institutional affiliations.

Ready to submit your research? Choose BMC and benefit from:

- fast, convenient online submission
- thorough peer review by experienced researchers in your field
- rapid publication on acceptance
- support for research data, including large and complex data types
- gold Open Access which fosters wider collaboration and increased citations
- maximum visibility for your research: over 100M website views per year

At BMC, research is always in progress.

Learn more biomedcentral.com/submissions

